HHS Public Access

Author manuscript

Biochem J. Author manuscript; available in PMC 2019 June 23.

Published in final edited form as:

Biochem J. 2012 February 15; 442(1): 95–103. doi:10.1042/BJ20111145.

Myosin regulatory light chain mutation found in hypertrophic cardiomyopathy patients increases isometric force production in transgenic mice

Katarzyna Kazmierczak, **Priya Muthu**, **Wenrui Huang**, **Michelle Jones**, **Yingcai Wang**, and **Danuta Szczesna-Cordary**[1]

Department of Molecular and Cellular Pharmacology, University of Miami Miller School of Medicine, Miami, FL 33136, U.S.A.

Abstract

FHC (familial hypertrophic cardiomyopathy) is a heritable form of cardiac hypertrophy caused by mutations in genes encoding sarcomeric proteins. The present study focuses on the A13T mutation in the human ventricular myosin RLC (regulatory light chain) that is associated with a rare FHC variant defined by mid-ventricular obstruction and septal hypertrophy. We generated heart-specific Tg (transgenic) mice with ~ 10 % of human A13T-RLC mutant replacing the endogenous mouse cardiac RLC. Histopathological examinations of longitudinal heart sections from Tg-A13T mice showed enlarged interventricular septa and profound fibrotic lesions compared with Tg-WT (wild-type), expressing the human ventricular RLC, or non-Tg mice. Functional studies revealed an abnormal A13T mutation-induced increase in isometric force production, no change in the force–pCa relationship and a decreased V_{max} of the acto-myosin ATPase. In addition, a fluorescence-based assay showed a 3-fold lower binding affinity of the recombinant A13T mutant for the RLC-depleted porcine myosin compared with WT-RLC. These results suggest that the A13T mutation triggers a hypertrophic response through changes in cardiac sarcomere organization and myosin cross-bridge function leading to abnormal remodelling of the heart. The significant functional changes observed, despite a low level of A13T mutant incorporation into myofilaments, suggest a ‘poison-peptide’ mechanism of disease.

Keywords

A13T mutation; ATPase activity; familial hypertrophic cardiomyopathy (FHC); fibrosis; muscle fibre force; myosin regulatory light chain (myosin RLC)

INTRODUCTION

FHC (familial hypertrophic cardiomyopathy) is an autosomal-dominant disorder caused by mutations in major sarcomeric proteins of the heart including the MHC (β-myosin heavy

[1]To whom correspondence should be addressed (dszczesna@med.miami.edu).

AUTHOR CONTRIBUTION

Katarzyna Kazmierczak, Priya Muthu, Wenrui Huang and Danuta Szczesna-Cordary designed the experiments and analysed the data. Yingcai Wang and Michelle Jones generated Tg A13T RLC mice. Katarzyna Kazmierczak, Priya Muthu and Wenrui Huang performed experiments. Katarzyna Kazmierczak, Priya Muthu, Michelle Jones and Danuta Szczesna-Cordary wrote the paper.

chain), myosin RLC (regulatory light chain) and ELC (essential light chain), myosin-binding protein C, Tm (tropomyosin), troponin (TnT, Tnl and TnC), actin and titin [1–6]. The disease typically presents with asymmetric LV (left ventricular) hypertrophy, myofilament disarray and myocardial fibrosis. The prevalence of FHC is approximately 0.2–0.5 % of the general population and it is considered the leading cause of SCD (sudden cardiac death), especially among athletes and young adults under 30 [7]. The A13T substitution in the myosin ventricular RLC was one of the first RLC mutations found in patients suffering from a rare variant of hypertrophic cardiomyopathy that involved massive hypertrophy of the papillary muscles and adjacent ventricular tissue causing a mid-cavity LV obstruction [8]. This mutation was later found to cause pronounced septal and ventricular hypertrophy and diastolic filling abnormalities [9,10].

The RLC binds to the myosin heavy chain IQ motif and together with the ELC supports the lever arm domain of the myosin head known to amplify small conformational changes originating at the myosin catalytic site into large movements needed to produce force and motion [11,12]. Mutations in the RLC may cause changes in the lever arm structure and/or function, thus leading to altered force generation and cardiac disease. Specifically, it is important to understand how the conformational change associated with the N-terminal A13T substitution in the myosin RLC can affect the interaction of RLC with the MHC and then mutant myosin with actin and ultimately the development of contractile force and heart performance.

The RLC is a member of a large EF-hand Ca^{2+} -binding protein family including TnC and CaM (calmodulin), and it is of interest to elucidate the potential Ca^{2+} -dependent alterations in tension production via RLC FHC-induced changes in the Ca^{2+}/Mg^{2+}-binding site (residues 37–48), and how they may affect muscle contraction [3,13]. Furthermore, the N-terminal domain of the human ventricular myosin RLC also contains the Ca^{2+}/CaM-activated MLCK (myosin light chain kinase) phosphorylation site at Ser^{15}, which is two amino acids away from the site of the FHC mutation at Ala^{13}. As we and other investigators have shown, phosphorylation of myosin RLC plays an important role in cardiac muscle contraction [14–19], and it is of great interest to investigate whether the A13T mutation affects RLC phosphorylation *in vivo* and consequently cardiac muscle function.

In the present study, we have generated heart-specific Tg (transgenic) mice expressing the human ventricular A13T-RLC mutation to elucidate the underlying mechanisms of this mutation, and to test whether specific functional and structural abnormalities observed in Tg-A13T mice could be correlated with clinical phenotypes [8–10]. Approximately 10 % of endogenous mouse cardiac RLC was replaced by the A13T mutant of human ventricular RLC in Tg-A13T mouse myocardium, whereas ~40 % and ~100 % of human ventricular RLC incorporation was achieved in Tg-WT (wild-type) mice. In agreement with phenotypes observed in humans, histopathology study on longitudinal heart sections from Tg-A13T mice showed enlarged interventricular septa and profound fibrotic lesions compared with Tg-WT or NTg (non-Tg) mice. Functional studies with Tg cardiac muscle preparations showed a 1.4-fold increase in maximal contractile force and a ~25 % decrease in the V_{max} of actin-activated myosin ATPase in Tg-A13T compared with Tg-WT or NTg mice. The molecular mechanisms responsible for these significant functional changes observed despite

a low level of incorporation of the A13T-RLC mutant into mouse cardiac sarcomeres are discussed below.

MATERIALS AND METHODS

Generation of Tg mice

All animal studies were conducted in accordance with institutional guidelines. The University of Miami has an Animal Welfare Assurance (A-3224–01, effective 11 July 2007) on file with the OLAW (Office of Laboratory Animal Welfare), National Institutes of Health. We have generated Tg mouse models of WT human ventricular RLC (NCBI accession no. P10916) [20] and the A13T mutation, shown by population studies to cause FHC [8–10]. The cDNA of the A13T-RLC protein was cloned into the unique Salí site of the plasmid, α-myosin heavy chain clone 26 (generously provided by Dr J. Robbins, Cincinnati Children's Hospital Medical Center, Cincinnati, OH, U.S.A.). The resulting constructs contained approximately 5.5 kb of the mouse a-myosin heavy chain promoter, including the first two exons and part of the third, followed by the A13T cDNA (498 bp) and a 630 bp 3′-untranslated region from the human growth hormone transcript [20]. All founders were bred to non-Tg B6SJL mice. Multiple crosses of Tg mice with B6SJL/F1 mice were performed before the animals were used for experiments.

Histopathological characterization

After killing, the hearts of ~6-month-old male mice from each group were excised and immersed in 10 % buffered formalin. Slides of whole mouse hearts were prepared by American Histolabs. The paraffin-embedded longitudinal and cross-sections of whole mouse hearts stained with H/E (haematoxylin and eosin) and Masson's trichrome were examined for overall morphology, hypertrophy and fibrosis using a Dialux 20 microscope, ×40/0.65 NA (numerical aperture) Leitz Wetzlar objective and an AxioCam HRc camera (Zeiss). Slides with H/E-stained longitudinal sections from NTg, Tg-WT and Tg-A13T mouse hearts were analysed for the number of nuclei. The nuclei count was taken from four segments of each slide (approximate area = 0.014 mm^2), averaged and expressed per mm^2. Five to eight slides from each group of mice were analysed.

Analysis of Tg protein expression

The α-MHC-driven expression of the human ventricular WT or A13T-RLC proteins in mouse hearts was quantified utilizing mouse atrial heart samples. The expression level was assessed on the basis of the greater gel mobility of the human ventricular RLC (18.7 kDa) compared with mouse atrial RLC (19.3 kDa) [20]. Approximately 10 mg of atrial tissue from Tg-A13T, Tg-WT and NTg mice of various ages and genders were minced in a solution consisting of 8 M urea, 10 mM Tris/HCl, pH 7.0, 1 % SDS, 1 % 2-mercaptoethanol, 1 mM EDTA, 1 mM PMSF and protease inhibitor cocktail (Sigma–Aldrich), homogenized, clarified by centrifugation at 18000 ***g*** for 10 min and quantified by a Coomassie-Plus Assay (Pierce). The extracts were loaded at 30 μg per lane, subjected to SDS/15 % PAGE and Coomassie Blue-stained, whereas approximately 20 μg per lane was electrophoresed for Western blotting. The Tg protein was detected using polyclonal anti-RLC CT-1 antibodies, with an epitope located in the C-terminus of the human ventricular RLC sequence (NCBI

accession no. P10916), produced in our laboratory, followed by a secondary goat anti-rabbit antibody conjugated with the fluorescent dye IR red 800 [20,21]. Total ELC (ELC of myosin) was detected with the monoclonal ab680 antibody (Abcam) followed by a secondary goat anti-mouse antibody conjugated with the fluorescent dye Cy 5.5. Blots were scanned and the respective bands were quantified using the Odyssey Infrared Imaging System (LI-COR).

Analysis of protein phosphorylation

After killing, the hearts from 5–6-month-old Tg-A13T, Tg-WT and NTg mice were excised and the ventricles were immediately isolated and frozen in liquid nitrogen. Prior to the experiment, the tissue was thawed and homogenized in a buffer consisting of 8 M urea, 10 mM Tris/HCl, pH 7.0,1 % SDS, 1 % 2-mercaptoethanol, 1 mM EDTA, 1 mM PMSF, 1 μl/ml protease inhibitor cocktail (Sigma) and 5 nM microcystin, and loaded on to SDS/15 % PAGE. The phosphorylated Tg RLC was detected with +P-RLC antibodies recognizing the phosphorylated form of the human or mouse ventricular RLC followed by a secondary goat anti-rabbit antibody conjugated with the fluorescent dye IR red 800. The total RLC protein was detected with a rabbit polyclonal RLC CT-1 antibody whereas the total ELC was detected with the ab680 antibody (as above), both of which served as loading controls.

Actin-activated myosin ATPase activity

Myosins isolated from the hearts of 3–5-month-old Tg-mice were purified as described previously [22,23]. Rabbit skeletal F-actin (filamentous actin) was prepared according to Kazmierczak et al. [23]. Actin-activated myosin ATPase activity was measured as a function of actin concentration and the data were analysed as described in detail in [23]. Briefly, 0.5 μM myosin dissolved in 0.4 M KCl (in monomeric form) was added to the 96-well microplate containing increasing concentrations of rabbit skeletal F-actin (in μM): 0.1, 5, 10, 15, 20 and 25. The assay was performed in a 120 μl reaction volume in a buffer consisting of 25 mM imidazole, pH 7.0, 4 mM $MgCl_2$, 1 mM EGTA and 1 mM DTT (dithiothreitol). The final KCl concentration was 107 mM. Protein mixtures were first incubated on ice for 10 min and then for another 10 min at 30 °C. The reactions (run in triplicate) were initiated with the addition of 2.5 mM ATP with mixing in a Jitterbug incubator shaker (Boekel), allowed to proceed for 15 min at 30 °C and then terminated by the addition of 5 % trichloroacetic acid. Precipitated proteins were cleared by centrifugation and the P_i was determined using the method of Fiske and Subbarow [24]. Data were analysed using the Michaelis–Menten equation, yielding V_{max} and K_m [25,26].

Skinned muscle fibres

The papillary muscles of the left ventricles from 5–6-month-old Tg female mice were isolated, dissected into muscle bundles and chemically skinned in 50 % glycerol and 50 % pCa 8 solution {10^{-8}MCa^{2+}, 1 mM free Mg^2 + [total MgPr (propionate) = 3.88 mM], 7 mM EGTA, 2.5 mM Mg-ATP$^-$, 20 mM Mops, pH 7.0, 15 mM creatine phosphate and 15 units/ml of creatine kinase, ionic strength = 150 mM adjusted with KPr} containing 1 % Triton X-100 for 24 h at 4 °C. Then the fibres were transferred to the same solution without Triton X-100 and stored at − 20 °C for approximately 5 days [21].

Steady-state force development

A bundle of approximately three or four single fibres isolated from a batch of glycerinated skinned mouse papillary fibres was attached by tweezer clips to a force transducer of the Guth muscle research system, placed in a 1 ml cuvette and freshly skinned in 1 % Triton X-100 dissolved in pCa 8 buffer for 30 min to remove the remaining membrane and ECM (extracellular matrix) proteins. Next the fibres were washed twice in pCa 8 buffer and tested for steady-state force development in pCa 4 solution (composition is the same as pCa 8 buffer except for the $[Ca^{2+}] = 10^{-4}$ M). Maximal steady-state force development was measured in Tg-A13T, Tg-WT and NTg fibres, and expressed in Newtons per cross-section of muscle fibre (kN/m^2), with the cross-sectional area assumed to be circular [27]. The measurement of fibre diameter was taken at ~3 points along the fibre length with an SZ6045 Olympus microscope (zoom ratio of 6.3:1, up to ×189 maximum magnification) and averaged [27]. Maximal tension developed by Tg-A13T muscle fibres was compared with controls, Tg-WT and NTg mice. All mechanical experiments on glycerinated skinned papillary muscle fibres were carried out at room temperature (22°C).

The Ca^{2+} dependence of force development

After the initial steady-state force was determined, the fibres were relaxed in pCa 8 buffer and then exposed to solutions of increasing Ca^{2+} concentration from pCa 8 to pCa 4 [28]. The maximal force was measured in each 'pCa' solution followed by a short relaxation of the fibres in pCa 8 solution. Data were analysed using the Hill equation [29], where $[Ca^{2+}]_{50}$ (pCa_{50}) is the free Ca^{2+} concentration that produces 50 % force, and h ('n_H') is the Hill coefficient.

Depletion of native RLC from porcine cardiac myosin and reconstitution with increasing concentrations of human cardiac WT-RLC or A13T-RLC mutant

Porcine cardiac myosin was purified as described by Pant et al. [30]. Recombinant human cardiac WT-RLC and A13T-RLC were expressed and purified as described by Szczesna et al. [31]. Endogenous native RLC was depleted from porcine myosin by incubation of myosin with 1 % Triton X-100 and 5 mM CDTA (1,2-cyclohexylenedinitrilotetra-acetic acid), pH 8.5, for 60 min at room temperature. The Triton/CDTA-treated myosin was then precipitated with 13 volumes of ice-cold water containing 1 mM DTT and was collected by centrifugation (8000 ***g*** at 4°C for 10 min). Myosin depleted of endogenous RLC was then resuspended in a buffer composed of 0.4 M KCl, 50 mM Mops, pH 7.0, 2 mM $MgCl_2$ and 1 mM DTT, and titrated with increasing concentrations of recombinant human cardiac RLC (WT or A13T) in the presence of BSA, used to prevent any non-specific RLC binding. The mixtures were incubated for 30 min at room temperature and left to precipitate in 13 volumes of ice-cold 1 mM DTT for 20 min. Protein complexes were then pelleted by centrifugation and separated by SDS/PAGE. Coomassie Blue- stained gels were scanned and the bands were quantified using the Odyssey Infrared Imaging System. The ELC of myosin, not extracted under experimental conditions used [30], served as a loading control and the ELC/RLC band ratios were used to determine the degree of reconstitution with A13T- and WT-RLC.

Fluorescence measurements

Rabbit skeletal actin was labelled with pyrene iodoacetamide (Invitrogen/Molecular Probes) as follows: F-actin was dissolved in the F-actin buffer, containing 10 mM Mops, 1 mM $MgCl_2$ and 40 mM KCl, pH 7, to a concentration of ~2 mg/ml and was allowed to react with an 8 M excess of pyrene [dissolved in DMF (dimethylformamide)], for 16 h in the dark at the room temperature with constant rotation. Then the reaction was quenched with 1 mM DTT and the preparation was centrifuged at 940 ***g*** for 1 h. Then F-actin was dialysed against G-actin buffer (5 mM Tris/HCl, pH 8.0, 0.2 mM $CaCl_2$ and 0.2 mM ATP), to remove excess pyrene, overnight at 4 °C. G-actin was dialysed against F-actin buffer to form F-actin at 4 °C for 4 h. The resulting molar ratio of pyrene/F-actin was 0.8, determined using the molar absorption coefficient (ε), ε_{344}(pyrene) = 22000 $M^{-1} \cdot cm^{-1}$. For these assays, the time of RLC-depletion in porcine myosin was decreased to 30 min, and the RLC-depleted myosin was then incubated on ice for 2 h with slow stirring with recombinant WT or A13T-RLCina 1:3 molar ratio. The WT- or A13T-reconstituted myosins were dialysed overnight against 5 mM DTT and used in actin-binding experiments. Pyrene-labelled F-actin at 0.5 μM (stabilized by 0.5 μM phalloidin), was titrated with increasing concentrations of A13T- or WT-reconstituted myosins in a 2 ml cuvette in a buffer containing 10 mM Mops and 0.4 M KCl, pH 7.0. Fluorescence was recorded with λ_{em} at 408 nm and with λ_{ex} at 340 nm using a FP-6500 fluorimeter (Jasco). The binding isotherms were fitted to the non-linear binding model:

$$y = m_1 - m_2 v$$

where m_1 is the fluorescence intensity at 0 pM myosin, m_2 is the fluorescence intensity at saturating myosin concentrations, and v *is the fractional saturation of binding sites and is a root of the quadratic equation:*

$$nav^2 - \left(K_d + na + b\right)v + b = 0$$

where a and b are the total concentrations of actin ($a = 0.5$ μM) and myosin respectively, n is the apparent stoichiometry and K_d is the apparent equilibrium dissociation constant [32].

Statistical analysis

Data are expressed as the average of n experiments ± S.E.M. Multiple comparisons between groups were performed using one-way ANOVA procedures and an unpaired Student's t test (Sigma Plot 11; Systat Software). The significance was defined as $P < 0.05$.

RESULTS

Two previously generated Tg mouse lines of Tg-WT expressing ~ 100 % (L2) and ~ 40 % (L4) of the human ventricular myosin RLC were used in these studies [20]. Tg-WT mice served as controls for the newly produced Tg-A13T mice (L1 and L2). Because of the low A13T-RLC expression in Tg-A13T L1 mice (see below), the NTg littermates were included

as additional control group in all experiments performed. Therefore all Tg-A13T results presented were compared with Tg-WT (L2 and L4) and NTg mice.

Histology

Histopathological evaluation of the hearts from Tg-A13T, Tg-WT and NTg mice is presented in Figure 1. As shown in Figure 1(A), a significantly larger IVS (inter-ventricular septal) mass was observed in longitudinal sections of H/E-stained whole hearts from representative 6-month-old Tg-A13T mice compared with Tg-WT or NTg littermates. High-magnification images of IVS and LV sections stained with H/E and Masson's trichrome are presented in Figures 1(B) and 1(C) respectively. The A13T animals demonstrated severe fibrotic lesions in their LV walls compared with controls suggesting exaggerated deposits of extracellular collagen (Figure 1C). In addition, the analysis of high-magnification images of H/E-stained IVS sections from the hearts of Tg mice from all groups (Figure 1B) revealed a significant decrease in the number of nuclei/mm^2 in Tg-A13T hearts compared with Tg-WT or NTg hearts (Figure 1D). A lower nuclei count per mm^2 in Tg-A13T heart sections indicates an A13T-induced hypertrophy leading to an increase in the two-dimensional size of myocytes compared with the two-dimensional images of myocytes from Tg-WT or NTg hearts. These findings demonstrate that the human phenotype of septal hypertrophy observed in patients harbouring this mutation [8–10] could be recapitulated in mice.

Analysis of protein expression and phosphorylation

The expression of the A13T mutant of RLC in Tg mouse L1 determined in mouse atrial extracts probed with CT-1 polyclonal anti-RLC antibodies [20] was 11.4 ± 1.8 % (n = 8 mice), whereas another Tg-A13T mouse line (L2) failed to produce any A13T-RLC protein (Figure 2A, upper panel). As with the R58Q and N47K FHC-linked RLC mutations studied previously [20], the α-MHC-driven expression of WT and A13T proteins was quantified utilizing mouse atrial heart samples. This is because there is very little difference in molecular mass between Tg human (P10916: M_W = 18.789 kDa) and endogenous mouse (P51667: M_W = 18.864 kDa) ventricular RLC resulting in no differential gel mobility of RLC in ventricular mouse samples (Figure 2A, lower panel, t-RLC_{ventr}. bands) preventing a direct assessment of the mutant protein in ventricles. However, a substantial difference in gel mobility is observed between Tg human ventricular RLC (WT or A13T) and the endogenous mouse atrial RLC (Q9QVP4: M_W = 19.450 kDa) allowing for a quantitative determination of transgene protein expression (Figure 2A, upper panel). Although a complete replacement of the endogenous mouse atrial RLC was observed in the myocardium of Tg-WT mice (Figure 2A, upper panel, lane 3), we could only achieve ~ 11 % replacement of the A13T mutant for the endogenous mouse atrial RLC in Tg-A13T L1 mice (Figure 2A, upper panel, lane 5). Figure 2(B) demonstrates the level of RLC phosphorylation determined in LV extracts of the rapidly frozen hearts from Tg-A13T against Tg-WT and NTg mice by SDS/PAGE and phospho-specific anti-RLC antibody [19] (Figure 2B, lower panel). As in Figure 2(A), total RLC protein in all mouse models shown in Figure 2(B) was probed with the anti-CT-1 antibody. Total ELC probed with the anti-ELC antibody was used as a loading control. As indicated, compared with NTg and Tg-WT mice, the endogenous RLC phosphorylation in Tg-A13T mice was not affected by the A13T mutation (Figure 2B, lane 2 compared with

lanes 1 and 3). This result, however, was somewhat expected after consideration of the very low level of A13T expression.

Actin-activated myosin ATPase activity assays

Myosin is an ATPase that converts chemical energy into directed movement powering muscle contraction [33]. The steady-state actin-activated myosin ATPase activities of Tg myosins purified from the mouse hearts were determined as a function of increasing F-actin concentrations (Figure 3). ATPase isotherms were obtained by plotting the ATPase activity against F-actin concentration, with data points expressed as means ± S.E.M. for four to five experiments. The data were fitted to the Michaelis-Menten equation yielding the V_{max} and K_m parameters. A significant decrease in V_{max} was observed in Tg-A13T mice (0.376 ± 0.016 s^{-1}) compared with Tg-WT (0.508 ± 0.012 s^{-1}) or NTg (0.627 ± 0.039 s^{-1}) mice (Figure 3). V_{max} represents the rate constant of the transition from the weakly (A · M · ATP↔ A · M · ADP · P_i) to strongly (A · M · ADP↔A · M) (A is actin, and M is myosin) bound myosin cross-bridges, with phosphate (P_i) release being rate-limiting [33]. Therefore the A13T mutation decreased the rate of the weak-to-strong actin- binding transition by 25 % and 40 % compared with Tg-WT and NTg myosins respectively (Figure 3). The K_m (dissociation constant) values between Tg-A13T (2.35 + 0.21 μM) and Tg-WT (2.00 ± 0.05 μM) or NTg (1.75 ± 0.32 μM) myosins were slightly different, but the differences were not statistically significant (Figure 3). Since the actin-activated hydrolysis of Mg-ATP by myosin fuels muscle contraction, these results suggest that the A13T mutation may affect the ability of the mutated crossbridges to hydrolyse ATP decreasing chemical energy that could be used to produce mechanical work.

Force development in skinned papillary muscle fibres

Cardiac muscle contraction is powered by the MgATP-dependent interaction of myosin with actin. To understand the effect of the A13T mutation in myosin RLC on force generation and to examine whether a reduced actin-activated myosin ATPase activity in Tg-A13T mice might affect average isometric force, we measured Ca^{2+} -dependent steady-state force development in skinned papillary muscle fibres from Tg-A13T against Tg-WT and NTg fibres. As shown earlier [20], the papillary muscle fibres were least affected by any FHC-linked RLC mutations as evaluated by histopathological changes in the mutated myocardium, and therefore were used in the functional studies. Any remaining extracellular collagen deposits were removed from the fibres during the process of skinning with 1 % Triton X-100 (see the Materials and methods section). The average length and diameter of the fibres used in the experiments were 1.2 ± 0.1mm and 105 ± 20 μm respectively (n ≈ 35 fibres). A large increase in maximal tension at pCa 4 was observed for Tg-A13T fibres (76.56 ± 2.51 kN/m^2, $n = 11$ fibres) compared with controls, Tg-WT (57.43 ± 0.16 kN/m^2, $n = 11$) or NTg (52.49 + 0.93 kN/m^2, $n = 5$) muscle fibres (Figure 4A). Statistical analysis of the cross-sectional area of Tg-A13T, Tg-WT or NTg fibres revealed no differences between the groups ($P > 0.05$), indicating that the observed increase in force in Tg-A13T against control fibres was due to a disease-causing mutation and not due to potential differences in cross-sectional area between the fibres from different mice. The increase in maximal tension was not accompanied by any changes in myofilament Ca^{2+} sensitivity and, as demonstrated in Figure 4(B), no significant differences in the pCa_{50} values of the force–pCa dependence

were observed between Tg-A13T fibres compared with Tg-WT and NTg fibres ($P > 0.05$). The midpoint pCa_{50} values were: Tg-A13T, 5.60 ± 0.01 ($n = 10$ fibres); Tg-WT, 5.59 ± 0.01 ($n = 11$); and NTg, 5.56 ± 0.01 ($n = 5$). The Hill coefficients were 3.16 ± 0.15 for Tg-A13T, 2.95 ± 0.08 for Tg-WT, and 3.69 ± 0.15 for NTg fibres showing the lowest co- operativity in the mutated Tg-A13T papillary muscle fibres.

Binding of A13T-RLC to RLC-depleted porcine myosin

To elucidate the basis of the 11.4 + 1.8 % (n = 8) incorporation of the A13T mutant into cardiac muscle sarcomeres in Tg-A13T mice compared with ~ 100 % (L2) or ~ 40 % (L4) of the WT in Tg-WT mice, we have studied the binding profiles of binding recombinant human cardiac WT and A13T proteins to the RLC-depleted porcine cardiac myosin. The CDTA/Triton-based treatment yielded ~ 90 % of endogenous RLC-free myosin. Myosin depleted of endogenous RLC was then titrated with increasing concentrations of recombinant WT or A13T and processed as described in the Materials and methods section. The band intensity ratios of the ELC to the RLC, in native (not extracted) and reconstituted myosins obtained from SDS/PAGE images were used to determine the degree of RLC reconstitution. Figure 5 demonstrates the averaged apparent K_d constants for A13T-RLC and WT-RLC. Compared with WT-RLC reconstituted myosin (K_d = 2.92 ± 0.45 μM, n = 13), the A13T mutant demonstrated ~ 3-fold decrease in the binding affinity to the RLC-depleted porcine myosin (K_d = 8.14 ± 0.95μM, n = 10). The difference between the apparent K_d values for A13T against WT was statistically significant ($P < 0.01$) (Figure 5). An observed lower binding affinity of the A13T mutant-RLC to its binding partner, the myosin heavy chain in the cardiac sarcomere may explain the observed low level of expression/incorporation of the A13T mutant protein in the hearts of Tg-A13T mice.

Binding of A13T-myosin to pyrene-actin

To test whether the A13T mutation affects the affinity of myosin to actin in a strong binding state, in rigor, we measured the binding of A13T-reconstituted myosin to rabbit skeletal F-actin fluorescently labelled with pyrene. As shown in Figure 6 (inset), the preparation of RLC-depleted myosin shows ~ 77 % of RLC removal (lane 2). Judging by the ELC/RLC band ratio in native myosin (lane 1), the RLC-depleted porcine myosin was fully reconstituted with either A13T-RLC (lane 4) or WT-RLC (lane 3) proteins. These A13T-or WT-reconstituted myosins were used in fluorescence-based binding assays to pyrene-actin performed under rigor conditions in 0.4 M KCl and 10 mM Mops, pH 7. As shown in Figure 6, the averaged binding isotherms for A13T-myosin overlapped with those for WT-myosin. The apparent dissociation constant (characteristic for strong binding state) was K_d = 24.4 ± 2.2 nM (n = 5) for A13T-myosin and K_d = 18.9 ± 1.7 nM (n = 7)for WT-myosin (Figure 6). There was a slight difference, indicating a lower affinity of A13T- compared with WT-myosin for actin, but it was not statistically significant. The stoichiometry 'n' of binding was 0.9 and 0.8 for A13T-myosin and WT-myosin respectively.

DISCUSSION

Hypertrophic cardiomyopathy is characterized by cardiac hypertrophy, myocyte disarray and interstitial fibrosis and is the most common cause of SCD in young people [34]. Although

the genetic bases of FHC are quite well documented and understood, the underlying mechanisms responsible for the clinical phenotypes remain unknown. In the present paper, we focus on a rare case of FHC associated with a defect in the *MYL2* (myosin light chain 2) gene, the A13T mutation in the ventricular myosin RLC. In humans, this A13T-RLC mutation was shown to cause a mid-LV obstruction due to massive hypertrophy of the cardiac papillary muscles and adjacent ventricular tissue [8]. Two later reports found the A13T-mutated patients to suffer from a profound septal hypertrophy, exertion induced dyspnoea and severe cardiac abnormalities which were enhanced by ergonomic exercise [9,10].

Muscle contraction and heart performance are powered by myosin, which consists of a tail region and two catalytic heads, each containing an actin-binding site, a converter domain and the ELC- and RLC-binding region [35]. Myosin is an actin-dependent molecular motor that binds ATP and actin and uses the chemical energy derived from ATP hydrolysis to produce mechanical work. The A13T mutation is located in the N-terminus of the myosin RLC, which together with the ELC support the neck region of the myosin head attaching to their respective IQ motifs [35]. The neck region of the myosin head connects the catalytic and actin-binding domains with the myosin filament backbone, and is thought to act as a lever arm amplifying conformational changes originated at the active site into large movements resulting in force generation [36–38]. It has been suggested that the interaction of the RLC with the motor domain of myosin is critical for the energy transduction process and the transition of the myosin cross-bridge from a pre-power stroke to post-power stroke configuration [33].

Given the unique position of the RLC within the lever arm domain and its active participation in the acto-myosin ATPase cycle, it is conceivable that a structural change brought about by the A13T mutation in the RLC could result in an abnormal myosin ATPase activity, decreased rates of Pj release and potential changes in the power stroke. Since the hydrolysis of ATP by myosin fuels muscle contraction, it is likely that the A13T mutation in the RLC interferes with the ability of myosin to hydrolyse ATP providing inadequate energy to support mechanical work. The slower rates of P_i release by the cycling A13T-mutated myosin cross-bridges (Figure 3) coincided with higher force measured at maximum activation (pCa 4) in Tg-A13T skinned papillary muscle fibres compared with controls (Figure 4A). The greater force produced by the A13T cross-bridges was not accompanied by any increase (or decrease) in the Ca^{2+} sensitivity of the force (Figure 4B). One can hypothesize that the structural change that occurs in the myosin lever arm (A13T substitution in RLC) is communicated to the myosin catalytic domain leading to a decreased rate of cross-bridge transition from their weakly to strongly bound configuration: V_{max} A · M · ATP↔ A · M · ADP · P_i V_{max} A ·M · ADP↔ A · M, where A is actin and M is myosin [33]. According to the hypothesis of the mechanism for muscle contraction proposed by Huxley [39], the transition from the non-force-generating states (A · M · ATP↔ A · M · ADP · P_i) to the force-generating states (A · M · ADP↔A · M) in muscle can be characterized by the cross-bridge attachment rate *f* and the return to the non-force-generating states by the cross-bridge detachment rate g. Consequently, the fraction of force-generating myosin cross-bridges attached at maximal Ca^{2+} activation can be characterized by *f*/(*f* + g) [40]. For the ratio *f*/(*f* + g) to remain constant or increased (higher pCa 4 force

with no change in force–pCa) with potentially decreased f in the A13T myocardium, the rate of cross-bridge dissociation g would have to decrease. On the basis of this model, we believe that the A13T mutation affects the myosin power stroke generation by changing the kinetic properties of the cross-bridges. Future studies using single-molecule detection, as we have done for other RLC mutations [41–43], are necessary to directly determine the effect of A13T mutation on the kinetics of cycling cross-bridges in Tg-A13T muscle preparations.

To test the molecular basis of the low (~ 10 %) incorporation of the A13T mutant protein in cardiac muscle sarcomeres of Tg- A13T mice, we have examined the binding affinity of recombinant human cardiac WT and A13T proteins to the RLC-depleted porcine cardiac myosin (Figure 5). A 3-fold decrease in the binding constant was observed for A13T-RLC compared with WT-RLC. Therefore the low level of A13T expression observed in Tg-A13T mice is most likely caused by a lower affinity of the mutant-RLC to MHC compared with WT-RLC. The low incorporation of the mutant protein into cardiac myofilaments in Tg-A13T mice raises a question regarding the potential of Tg-A13T myocardium to develop significantly higher force than NTg or WT controls. The major mechanism accounting for the functional phenotype in dominant disorders such as FHC, is believed to be that of a dominant-negative (also called poison-peptide) effect [44]. In Tg-A13T mouse myocardium both proteins are expressed, the endogenous RLC (normal allele) and the mutant RLC (A13T-Tg allele); however, the mutant protein functions as a poison peptide that changes the function of the normal protein, leading to disease. Similar effects were observed with other FHC-linked sarcomeric mutations expressed in mice, e.g. TnT [45] and Tnl [46], where despite relatively low levels of expression (below 10 %), the incorporation of mutant protein induced myofilament disarray, profound fibrotic lesions and functional abnormalities. As with our A13T mutation, the observed phenotypes associated with these troponin mutations were essentially the same as those observed in humans. Then we can conclude that A13T-RLC exerted a dominant-negative effect on cardiac myocyte structure and function in patients carrying this mutation [8] and in Tg mice (Figures 1, 3 and 4).

It is now becoming evident that the most promising approaches to alleviate or reverse detrimental disease phenotypes must emerge from target-specific interventions determined by the functional phenotype [47]. The A13T-phenotype described in this report differs from other FHC-linked RLC mutations described in our previous studies. For example, the R58Q and D166V RLC-mutations associated with malignant disease outcomes had a profound effect on calcium homoeostasis and both increased the Ca^{2+} -sensitivity of contraction [17,20,48], whereas no changes in force/ATPase-pCa relationship were observed in this study. However, similarly to R58Q and D166V, it is believed that an A13T-induced decrease in g (myosin cross-bridge kinetics) is responsible for abnormal contractile force even though the force was decreased in Tg-R58Q and Tg-D166V mice, whereas it was increased in Tg-A13T myocardium [48,49]. Other phenotypic differences between these FHC-linked RLC mutations were observed in the levels of endogenous RLC phosphorylation. Both mutations, R58Q and D166V, led to a decreased RLC phosphorylation [17,27,41,48], whereas no change in phosphorylation of RLC was observed in Tg-A13T myocardium. Perhaps, the effect of FHC mutation on RLC phosphorylation underlines the mechanism of force generation in these different RLC animal models of FHC. Together results from previous and current studies on FHC-linked mutations in myosin RLC lead to the conclusion that

therapeutic efforts should be focused on restoring the normal level of contractile force in FHC-diseased hearts to return their normal systolic and diastolic functions.

ACKNOWLEDGEMENTS

We thank Dr Olga M. Hernandez for her work with the Tg-A13T construct. We greatly appreciate the gift of phospho-RLC antibody from Dr Neal Epstein (National Institutes of Health, Bethesda, MD, U.S.A.). We also thank Ana Rojas for her excellent technical assistance with Tg mice.

FUNDING

This work was supported by the National Institutes of Health [grant numbers HL071778 and HL090786 (to D.S.-C)] and the American Heart Association [grant number 10POST3420009 (to P.M.)].

Abbreviations used

CaM	calmodulin
CDTA	1,2-cyclohexylenedinitrilotetra-acetic acid
DTT	dithiothreitol
ELC	essential light chain
F-actin	filamentous actin
FHC	familial hypertrophic cardiomyopathy
H/E	haematoxylin and eosin
IVS	inter-ventricular septal
LV	left ventricular
MHC	β-myosin heavy chain
NTg	non-transgenic
RLC	regulatory light chain
SCD	sudden cardiac death
Tg	transgenic
Tn	troponin
WT	wild-type

REFERENCES

1. Seidman CE and Seidman JG (1998) Molecular genetic studies of familial hypertrophic cardiomyopathy. Basic Res. Cardiol 93,13–16 [PubMed: 9879437]
2. Maron BJ (2002) Hypertrophic cardiomyopathy: a systematic review. JAMA, J. Am. Med. Assoc 287,1308–1320
3. Szczesna D (2003) Regulatory light chains of striated muscle myosin. Structure, function and malfunction. Curr. Drug Targets Cardiovasc. Haematol. Disord 3,187–197 [PubMed: 12769642]

4. Tardiff J (2005) Sarcomeric proteins and familial hypertrophic cardiomyopathy: linking mutations in structural proteins to complex cardiovascular phenotypes. Heart Fail. Rev 10, 237–248 [PubMed: 16416046]
5. Hernandez OM, Jones M, Guzman G and Szczesna-Cordary D (2007) Myosin essential light chain in health and disease. Am. J. Physiol. Heart Circ. Physiol 292, H1643–H1654 [PubMed: 17142342]
6. Alcalai R, Seidman JG and Seidman CE (2008) Genetic basis of hypertrophic cardiomyopathy: from bench to the clinics. J. Cardiovasc. Electrophysiol 19,104–110 [PubMed: 17916152]
7. Spirito P, Bellone P, Harris KM, Bernabo P, Bruzzi P and Maron BJ (2000) Magnitude of left ventricular hypertrophy and risk of sudden death in hypertrophic cardiomyopathy. N. Engl. J. Med 342,1778–1785 [PubMed: 10853000]
8. Poetter K, Jiang H, Hassanzadeh S, Master SR, Chang A, Dalakas MC, Rayment I, Sellers JR, Fananapazir L and Epstein ND (1996) Mutations in either the essential or regulatory light chains of myosin are associated with a rare myopathy in human heart and skeletal muscle. Nat. Genet 13, 63–69 [PubMed: 8673105]
9. Andersen PS, Havndrup O, Bundgaard H, Moolman-Smook JC, Larsen LA, Mogensen J, Brink PA, Borglum AD, Corfield VA, Kjeldsen K et al. (2001) Myosin light chain mutations in familial hypertrophic cardiomyopathy: phenotypic presentation and frequency in Danish and South African populations. J. Med. Genet 38, E43 [PubMed: 11748309]
10. Hougs L, Havndrup O, Bundgaard H, Kober L, Vuust J, Larsen LA, Christiansen M and Andersen P S. (2005) One third of Danish hypertrophic cardiomyopathy patients have mutations in MYH7 rod region. Eur. J. Hum. Genet 13,161–165 [PubMed: 15483641]
11. Rayment I, Holden HM, Whittaker M, Yohn CB, Lorenz M, Holmes KC and Milligan RA (1993) Structure of the actin-myosin complex and its implications for muscle contraction. Science 261, 58–65 [PubMed: 8316858]
12. Geeves MA and Holmes KC (1999) Structural mechanism of muscle contraction. Annu. Rev. Biochem 68, 687–728 [PubMed: 10872464]
13. Szczesna-Cordary D, Guzman G, Ng SS and Zhao J (2004) Familial hypertrophic cardiomyopathy-linked alterations in Ca^2 + binding of human cardiac myosin regulatory light chain affect cardiac muscle contraction. J. Biol. Chem 279, 3535–3542 [PubMed: 14594949]
14. Ding P, Huang J, Battiprolu PK, Hill JA, Kamm KE and Stull JT (2010) Cardiac myosin light chain kinase is necessary for myosin regulatory light chain phosphorylation and cardiac performance *in vivo*. J. Biol. Chem. 285,40819–40829 [PubMed: 20943660]
15. Colson BA, Locher MR, Bekyarova T, Patel JR, Fitzsimons DP, Irving TC and Moss RL (2010) Differential roles of regulatory light chain and myosin binding protein-C phosphorylations in the modulation of cardiac force development. J. Physiol 588, 981–993 [PubMed: 20123786]
16. Doroszko A, Polewicz D, Cadete VJ, Sawicka J, Jones M, Szczesna-Cordary D, Cheung PY and Sawicki G (2010) Neonatal asphyxia induces the nitration of cardiac myosin light chain 2 that is associated with cardiac systolic dysfunction. Shock 34, 592–600 [PubMed: 20386496]
17. Abraham TP, Jones M, Kazmierczak K, Liang H-Y, Pinheiro AC, Wagg CS, Lopaschuk GD and Szczesna-Cordary D (2009) Diastolic dysfunction in familial hypertrophic cardiomyopathy transgenic model mice. Cardiovasc. Res 82, 84–92 [PubMed: 19150977]
18. Huang J, Shelton JM, Richardson JA, Kamm KE and Stull JT (2008) Myosin regulatory light chain phosphorylation attenuates cardiac hypertrophy. J. Biol. Chem 283,19748–19756 [PubMed: 18474588]
19. Davis JS, Hassanzadeh S, Winitsky S, Lin H, Satorius C, Vemuri R, Aletras AH, Wen H and Epstein ND (2001) The overall pattern of cardiac contraction depends on a spatial gradient of myosin regulatory light chain phosphorylation. Cell 107, 631–641 [PubMed: 11733062]
20. Wang Y, Xu Y, Kerrick WGL, Wang Y, Guzman G, Diaz-Perez Z and Szczesna-Cordary D (2006) Prolonged Ca^2 + and force transients in myosin RLC transgenic mouse fibers expressing malignant and benign FHC mutations. J. Mol. Biol 361,286–299 [PubMed: 16837010]
21. Szczesna-Cordary D, Guzman G, Zhao J, Hernandez O, Wei J and Diaz-Perez Z (2005) The E22K mutation of myosin RLC that causes familial hypertrophic cardiomyopathy increases calcium sensitivity of force and ATPase in transgenic mice. J. Cell Sci 118, 3675–3683 [PubMed: 16076902]

22. Szczesna-Cordary D, Jones M, Moore JR, Watt J, Kerrick WGL, Xu Y, Wang Y, Wagg C and Lopaschuk GD (2007) Myosin regulatory light chain E22K mutation results in decreased cardiac intracellular calcium and force transients. FASEB J. 21, 3974–3985 [PubMed: 17606808]
23. Kazmierczak K, Xu Y, Jones M, Guzman G, Hernandez OM, Kerrick WGL and Szczesna-Cordary D (2009) The role of the N-terminus of the myosin essential light chain in cardiac muscle contraction. J. Mol. Biol 387, 706–725 [PubMed: 19361417]
24. Fiske CH and Subbarow Y (1925) The colorimetric determination of phosphorus. J. Biol. Chem. 66, 375–400
25. Hanson KR, Ling R and Havir E (1967) A computer program for fitting data to the Michaelis-Menten equation. Biochem. Biophys. Res. Commun 29,194–197 [PubMed: 6066278]
26. Trybus KM (2000) Biochemical studies of myosin. Methods 22, 327–335 [PubMed: 11133239]
27. Muthu P, Kazmierczak K, Jones M and Szczesna-Cordary D (2011) The effect of myosin RLC phosphorylation in normal and cardiomyopathic mouse hearts. J. Cell. Mol. Med, doi: 10.1111/j.1582-4934.2011.01371.x
28. Dweck D, Reyes-Alfonso A Jr and Potter JD (2005) Expanding the range of free calcium regulation in biological solutions. Anal. Biochem 347, 303–315 [PubMed: 16289079]
29. Hill TL, Einsenberg E and Greene LE (1980) Theoretical model for the cooperative equilibrium binding of myosin subfragment-1 to the actin-troponin-tropomyosin complex. Proc. Natl. Acad. Sci. U.S.A. 77, 3186–3190 [PubMed: 10627230]
30. Pant K, Watt J, Greenberg M, Jones M, Szczesna-Cordary D and Moore JR (2009) Removal of the cardiac myosin regulatory light chain increases isometric force production. FASEB J. 23, 3571–3580 [PubMed: 19470801]
31. Szczesna D, Ghosh D, Li Q, Gomes AV, Guzman G, Arana C, Zhi G, Stull JT and Potter JD (2001) Familial hypertrophic cardiomyopathy mutations in the regulatory light chains of myosin affect their structure, Ca^{2+} binding, and phosphorylation. J. Biol. Chem 276, 7086–7092 [PubMed: 11102452]
32. Lu X, Kazmierczak K, Jiang X, Jones M, Watt J, Helfman DM, Moore JR, Szczesna-Cordary D and Lossos IS (2011) Germinal center-specific protein human germinal center associated lymphoma directly interacts with both myosin and actin and increases the binding of myosin to actin. FEBS J. 278,1922–1931 [PubMed: 21447067]
33. Rayment I (1996) The structural basis of the myosin ATPase activity. J. Biol. Chem 271, 15850–15853 [PubMed: 8663496]
34. Maron BJ, Doerer JJ, Haas TS, Tierney DM and Mueller FO (2009) Sudden deaths in young competitive athletes: analysis of 1866 deaths in the United States, 1980–2006. Circulation 119,1085–1092 [PubMed: 19221222]
35. Rayment I, Rypniewski WR, Schmidt-Base K, Smith R, Tomchick DR, Benning MM, Winkelmann DA, Wesenberg G and Holden HM (1993) Three-dimensional structure of myosin subfragment-1: a molecular motor. Science 261, 50–58 [PubMed: 8316857]
36. Huxley HE (1969) The Mechanism of Muscular Contraction. Science 164,1356–1366 [PubMed: 4181952]
37. Geeves MA (2002) Molecular motors: Stretching the lever-arm theory. Nature 415, 129–131 [PubMed: 11805818]
38. Spudich JA and Sivaramakrishnan S (2010) Myosin VI: an innovative motor that challenged the swinging lever arm hypothesis. Nat. Rev. Mol. Cell Biol 11,128–137 [PubMed: 20094053]
39. Huxley AF (1957) A hypothesis for the mechanism of contraction of muscle. Prog. Biophys. Biophys. Chem 7, 255–318 [PubMed: 13485191]
40. Brenner B (1988) Effect of Ca^{2+} on Cross-bridge turnover kinetics in skinned single rabbit psoas fibers: implications for regulation of muscle contraction. Proc. Natl. Acad. Sci. U.S.A 85, 3265–3269 [PubMed: 2966401]
41. Muthu P, Mettikolla P, Calander N, Luchowski R, Gryczynski I, Gryczynski Z, Szczesna-Cordary D and Borejdo J (2010) Single molecule kinetics in the familial hypertrophic cardiomyopathy D166V mutant mouse heart. J. Mol. Cell. Cardiol 48, 989–998 [PubMed: 19914255]

42. Mettikolla P, Calander N, Luchowski R, Gryczynski I, Gryczynski Z and Borejdo J (2010) Kinetics of a single cross-bridge in familial hypertrophic cardiomyopathy heart muscle measured by reverse Kretschmann fluorescence. J. Biomed. Opt 15,017011 [PubMed: 20210485]

43. Mettikolla P, Luchowski R, Gryczynski I, Gryczynski Z, Szczesna-Cordary D and Borejdo J (2009) Fluorescence lifetime of actin in the familial hypertrophic cardiomyopathy transgenic heart. Biochemistry 48,1264–1271 [PubMed: 19159226]

44. Roberts R and Sigwart U (2001) New concepts in hypertrophic cardiomyopathies, part I. Circulation 104,2113–2116 [PubMed: 11673355]

45. Oberst L, Zhao G, Park JT, Brugada R, Michael LH, Entman ML, Roberts R and Marian AJ (1998) Dominant-negative effect of a mutant cardiac troponin T on cardiac structure and function in transgenic mice. J. Clin. Invest 102,1498–1505 [PubMed: 9788962]

46. Wen Y, Xu Y, Wang Y, Pinto JR, Potter JD and Kerrick WG (2009) Functional effects of a restrictive-cardiomyopathy-linked cardiac troponin I mutation (R145W) in transgenic mice. J. Mol. Biol 392,1158–1167 [PubMed: 19651143]

47. Marian AJ (2009) Experimental therapies in hypertrophic cardiomyopathy. J. Cardiovasc. Transl. Res 2, 483–492 [PubMed: 20560006]

48. Kerrick WGL, Kazmierczak K, Xu Y, Wang Y and Szczesna-Cordary D (2009) Malignant familial hypertrophic cardiomyopathy D166V mutation in the ventricular myosin regulatory light chain causes profound effects in skinned and intact papillary muscle fibers from transgenic mice. FASEB J. 23,855–865 [PubMed: 18987303]

49. Mettikolla P, Calander N, Luchowski R, Gryczynski I, Gryczynski Z, Zhao J, Szczesna-Cordary D and Borejdo J (2011) Cross-bridge kinetics in myofibrils containing familial hypertrophic cardiomyopathy R58Q mutation in the regulatory light chain of myosin. J. Theor. Biol 284, 71–81 [PubMed: 21723297]

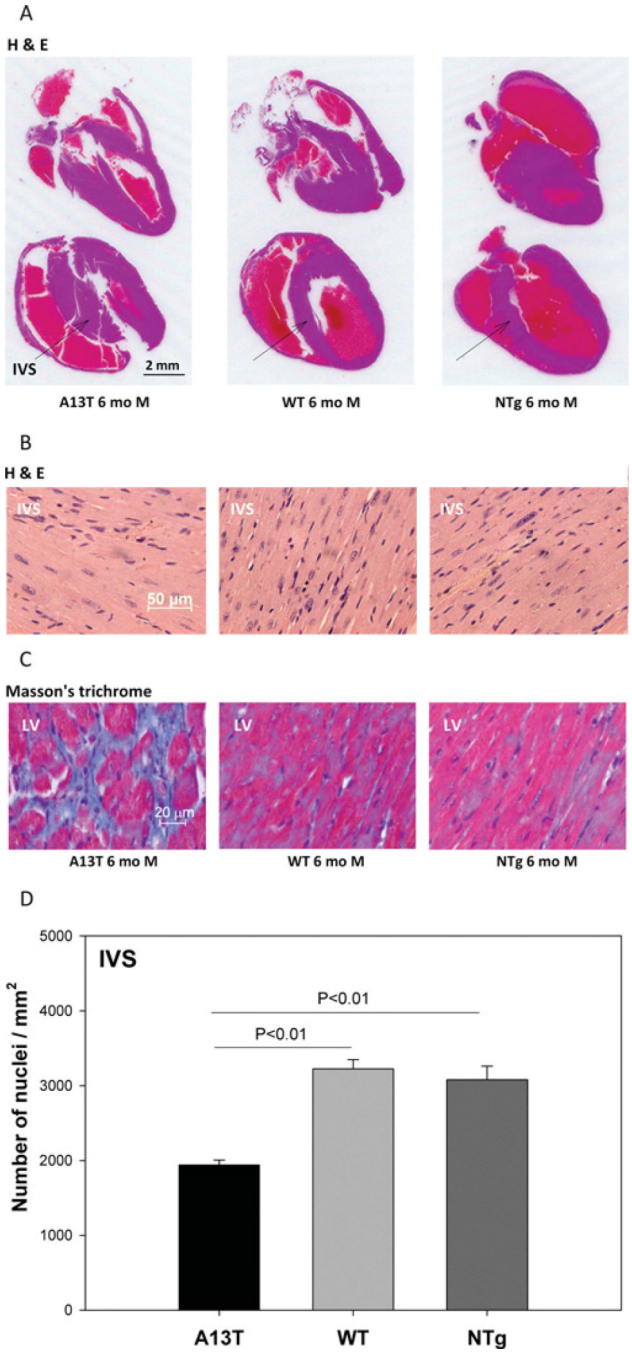

Figure 1. The effect of A13T mutation on heart morphology in Tg mice

After killing, the hearts from ~ 6-month (mo)-old male (M) Tg-A13T, Tg-WT and NTg mice were excised and immersed in 10% buffered formalin. (**A**) Longitudinal sections of whole mouse hearts stained with H/E for overall morphology. (**B**) High-magnification images of H/E-stained IVS for evaluation of heart morphology and assessment of nuclei. (**C**) High-magnification LV sections stained with Masson's trichrome for the evaluation of fibrosis. (**D**) Nuclei counts in the IVS sections from Tg-A13T, Tg-WT and NTg mouse hearts.

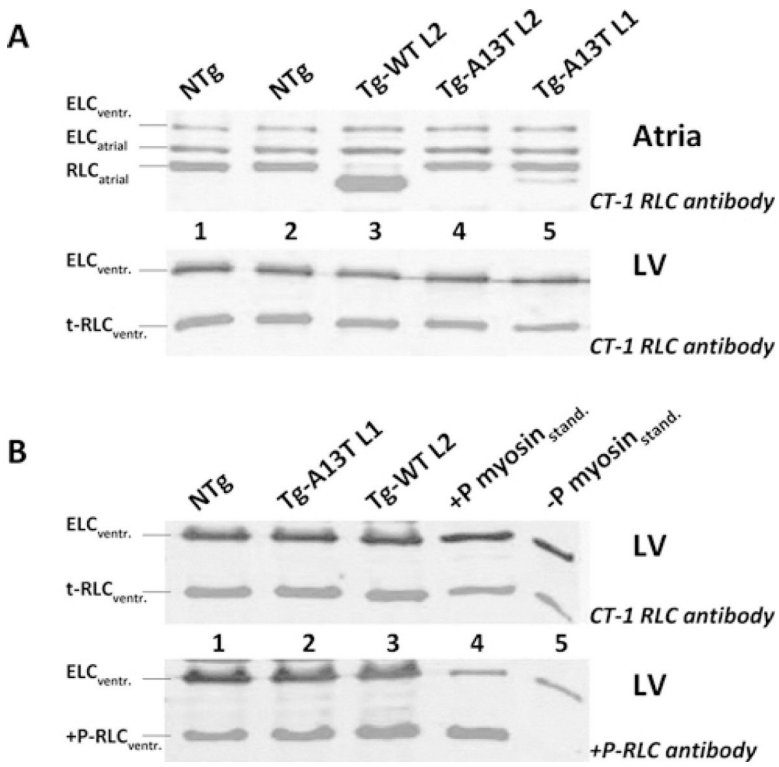

Figure 2. SDS/PAGE of Tg cardiac extracts

(**A**) Expression of A13T-RLC in Tg mice. Upper panel: expression in atria. Lower panel: expression in LV. Lanes 1 and 2, NTg extract; lane 3, Tg-WT L2 expressing ~ 100% of the human ventricular myosin RLC [20]; lane 4, Tg-A13T L2; and lane 5, Tg-A13T L1. (**B**) Analysis of RLC phosphorylation in LV of Tg-mice. Upper panel: total ventricular RLC (t-$RLC_{ventr.}$) detected with CT-1 RLC; lower panel, phosphorylated ventricular RLC (+ P-RLC_{ventr}) detected with + P-RLC antibody. Lane 1, NTg extract; lane 2, Tg-A13T L1; lane 3, Tg-WT L2; lanes 4 and 5, phosphorylated (+ P) and non-phosphorylated (− P) myosin protein standard ($myosin_{stand}$).

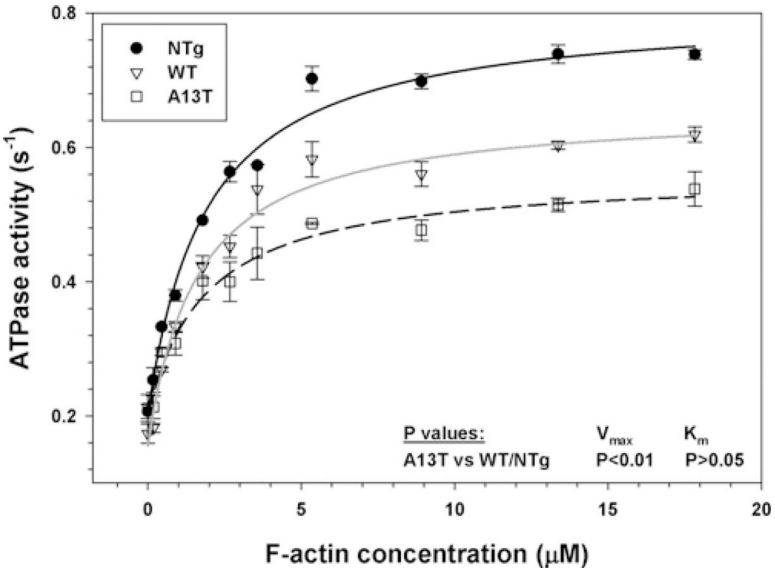

Figure 3. Actin-activated myosin ATPase activity

Measurements were performed on myosin isolated from left and right ventricles of 3–5-month-old Tg-A13T, Tg-WT L4 and NTg mice. A pool of approximately six or seven hearts from each group was used to obtain myosin preparations used in four or five independent experiments run in triplicate. Note a significantly lower V_{max} for A13T mouse myosin compared with WT or NTg mouse cardiac myosins.

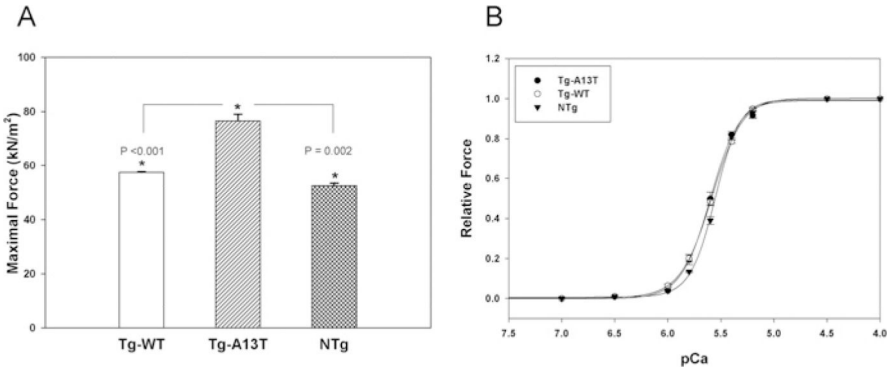

Figure 4. Maximal steady-state force (A) and force–pCa measurements (B) in Tg-A13T, Tg-WT and NTg skinned muscle fibres

A 30% increase in maximal force (expressed per cross-sectional area of muscle fibres) was observed for Tg-A13T mice compared with controls, Tg-WT or NTg (**A**). The increase in maximal force was not accompanied by any changes in the force–pCa dependence, and no significant differences in the pCa_{50} values were observed between Tg-A13T and control fibres (**B**). The data were derived from measurements on 5–11 individual skinned muscle fibres. * indicates significant differences in force between Tg-A13T and control mice.

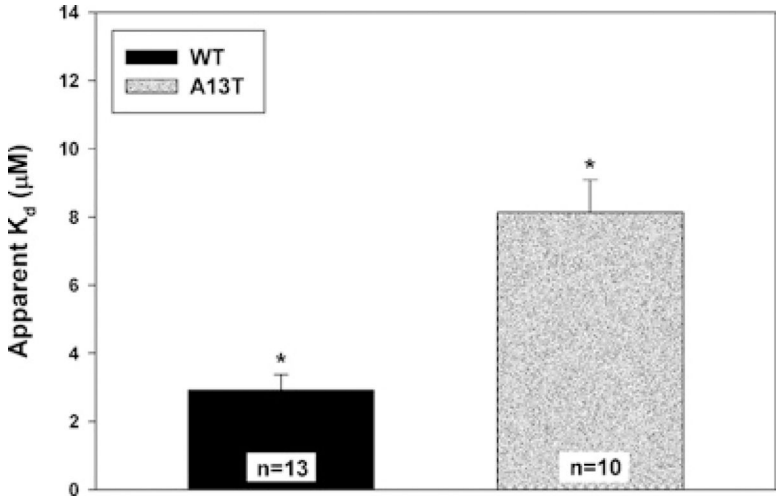

Figure 5. Apparent K_d constants of binding of the recombinant human cardiac RLC (WT) and the A13T-mutant to RLC-depleted porcine cardiac myosin

The difference in K_d between WT and A13T was statistically significant (*P< 0.01).

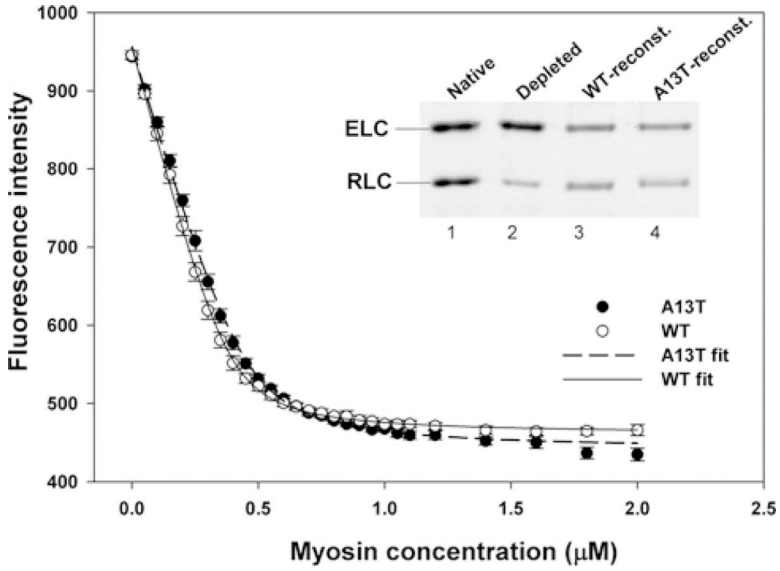

Figure 6. Binding of WT- and A13T-reconstituted porcine myosin to pyrene-labelled F-actin under rigor conditions

Association of myosin with actin resulted in quenching of pyrene fluorescence. The binding isotherms were fitted to a non-linear binding model as explained in the Materials and methods section. Inset: SDS/PAGE of RLC-depleted myosin (lane 2), used for reconstitution (reconst.) with the recombinant WT and A13T-RLC proteins (lanes 3 and 4). Lane 1 depicts native porcine myosin.